

## Breaking the Excitation Barrier: Visible-Light-Harvesting Ir(III)–Eu(III) Dyads for Circularly Polarized Luminescence and Theranostics

Zhiming Wang,<sup>a,b</sup> Shiwei Dong,<sup>a,b</sup> Chuanliang Yang,<sup>a,b</sup> Jinyi Chen,<sup>a,b</sup> Wentao Wang,<sup>\*a</sup> Tao Li,<sup>\*a,b</sup> Guoqiang Yang,<sup>\*a,b,c</sup> and Zhong Han<sup>\*a,b</sup>

---

<sup>a</sup>. Postgraduate training base Alliance of Wenzhou Medical University, Wenzhou 325035, China. E-mail: wangwentao@wiucas.ac.cn; lita@ucas.ac.cn; gqyang@iccas.ac.cn; z\_han@wiucas.ac.cn

<sup>b</sup>. Wenzhou Institute, University of Chinese Academy of Sciences, Wenzhou, Zhejiang 325000, China

<sup>c</sup>. Key Laboratory of Photochemistry, Institute of Chemistry, Chinese Academy of Sciences, Beijing 100190, China

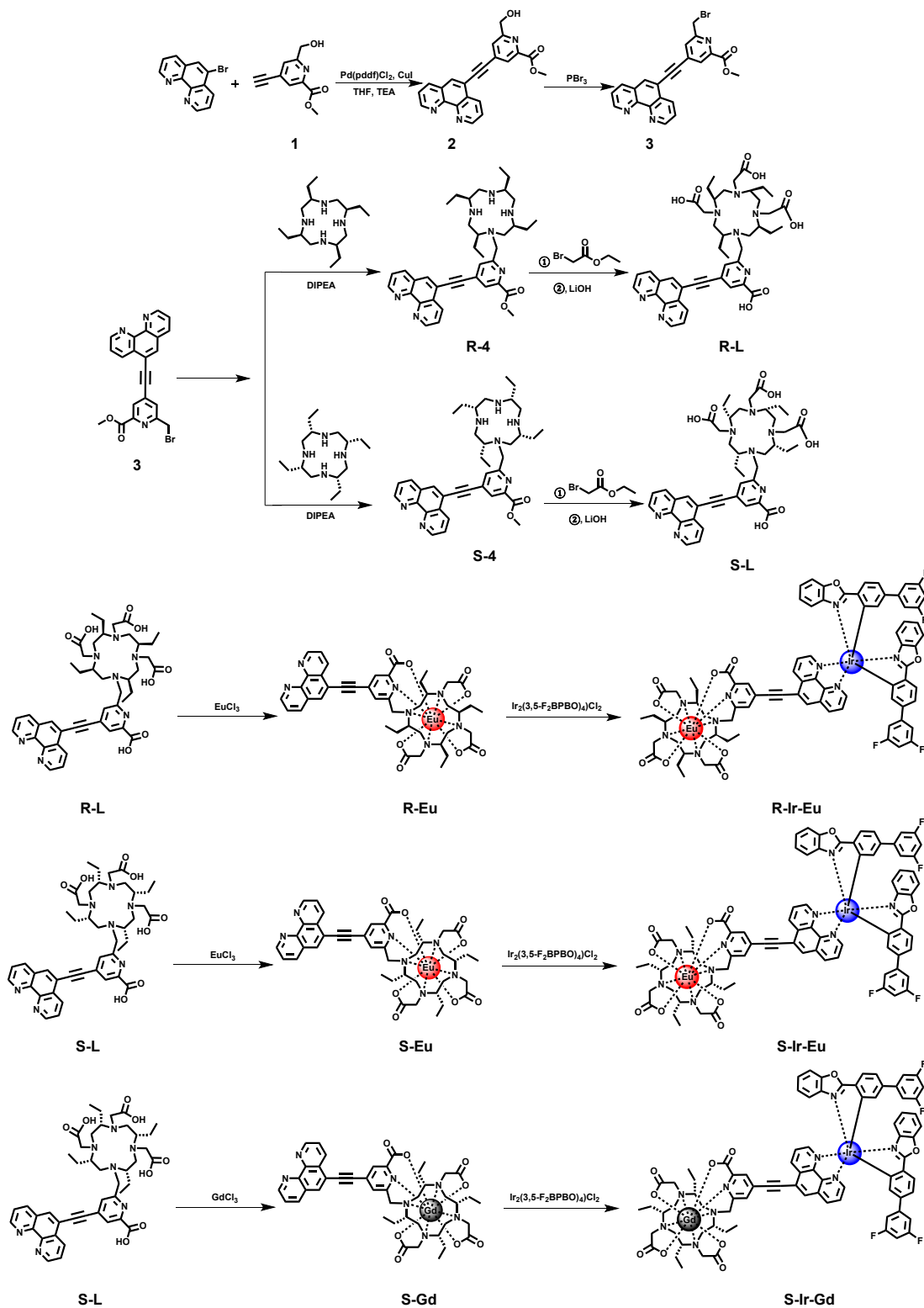
## Experimental section

**General procedures:** All operations were carried out under a pure argon atmosphere using standard Schlenk techniques. All reagents were purchased from commercial sources and used without further purification. All other chemical reagents of analytical grade were used directly without further purification.

The  $^1\text{H}$  NMR and  $^{13}\text{C}$  NMR spectra were recorded on a QUANTUM-I-400 at 298 K using deuterated solvents. Chemical shifts are given in ppm, and are referenced against internal TMS. High resolution mass spectrometric data were determined using an Agilent LTQ Orbitrap XL mass spectrometer. Fluorescence spectra were determined using a FluoroMax-4 spectrofluorometer (HORIBA) with a 5 nm slit for both excitation and emission. Lifetime was acquired through a time-correlated single photon counting (TCSPC) technique by using a HORIBA Jobin Yvon Fluorolog-3 modular spectrofluorometer. Absorption spectra were recorded using a Shimadzu UV-1900i spectrophotometer. All pH measurements of media were accomplished using a Model PHS-3C meter. Confocal luminescence images were captured in the confocal laser scanning microscopy (CLSM, Nikon A1 microscope). Circularly Polarized Luminescence (CPL) spectra were measured on a JASCO CPL-300 spectropolarimeter.

## Synthetic procedures

The intermediate precursors were synthesized according to our established procedures.<sup>[1]</sup> The spectroscopic data matched well with the literature values, and their high purities were confirmed prior to the subsequent coordination reactions.



**Synthesis and characterization of R-Eu:** Ligand **R-L** (86 mg, 0.108 mmol) and europium(III) chloride hexahydrate ( $\text{EuCl}_3 \cdot 6\text{H}_2\text{O}$ , 44 mg, 0.118 mmol, 1.1 equiv.) were suspended in deionized water (5 mL). The pH of the resulting mixture was carefully adjusted to approximately 7.0 using dilute aqueous NaOH or HCl. The reaction mixture was then heated to reflux and magnetically stirred for 16 h. Upon completion, the mixture was allowed to cool to ambient temperature. The crude solution was filtered to remove any insoluble residues and subsequently purified by semi-preparative high-performance liquid chromatography. The fractions containing the pure product were collected and lyophilized to afford the target complex **R-Eu** as a pale yellow solid (50 mg, yield: 57.7%). HRMS (negative mode,  $m/z$ ): Calcd. 944.2855, found 944.2851 for  $[\text{M}]^-$ .

**Synthesis and characterization of R-Ir-Eu:** Under nitrogen atmosphere, the iridium(III) chloride-bridged dimer  $\text{Ir}_2(3,5\text{-F}_2\text{BPBO})_4\text{Cl}_2$  [2] (78 mg, 0.047 mmol) and the mononuclear complex **R-Eu** (78 mg, 0.094 mmol, 2.0 equiv.) were dissolved in a degassed solvent mixture of  $\text{CH}_2\text{Cl}_2$  and  $\text{CH}_3\text{OH}$  (12 mL, 2:1, v/v). The reaction mixture was heated to reflux and magnetically stirred for 6 h. Upon completion of the cleavage and coordination processes, the solution was cooled to room temperature, and the solvents were completely removed under reduced pressure. The resulting crude residue was purified by silica gel column chromatography to afford the final heterobimetallic dyad **R-Ir-Eu** as a yellow solid. ( $\text{C}_{81}\text{H}_{69}\text{EuF}_4\text{IrN}_9\text{O}_{10}$ , 46 mg, 28%). HR-MS (positive mode,  $m/z$ ): Calcd. 1750.4018, found 1750.4008 for  $[(\text{M}+\text{H})]^+$ . Elemental Analysis: Calcd. C, 55.60; H, 4.03; N, 7.20, found C, 55.72; H, 4.13; N, 7.11.

**Synthesis and characterization of S-Eu:** The chiral complex **S-Eu** was synthesized and purified following the identical procedure described above for **R-Eu**, except that the enantiomeric ligand **S-L** was used instead of **R-L**. The final product was obtained as a pale yellow solid (46 mg, yield: 53.1%). HRMS (negative mode,  $m/z$ ): Calcd. 944.2855, found 944.2834 for  $[\text{M}]^-$ .

**Synthesis and characterization of S-Ir-Eu:** The enantiomeric heterobimetallic dyad **S-Ir-Eu** was synthesized and purified following the identical procedure described above for **R-Ir-Eu**, except that the mononuclear complex **S-Eu** was used instead of **R-Eu**. The final product was obtained as a yellow solid ( $\text{C}_{81}\text{H}_{69}\text{EuF}_4\text{IrN}_9\text{O}_{10}$ , 40 mg, yield: 24%). HR-MS (positive mode,  $m/z$ ): Calcd. 1750.4018, found 1750.4027 for  $[(\text{M}+\text{H})]^+$ . Elemental Analysis: Calcd. C, 55.60; H, 4.03; N, 7.20, found C, 55.67; H, 4.10; N, 7.21.

**Synthesis and characterization of S-Gd:** The chiral complex **S-Gd** was synthesized and purified following the identical procedure described above for **S-Eu**, except that gadolinium(III) chloride hexahydrate was used instead of europium(III) chloride hexahydrate. The final product was obtained as a pale yellow solid (57 mg, yield: 56%). HRMS (negative mode,  $m/z$ ): Calcd. 949.2889, found 949.2901 for [M]<sup>-</sup>).

**Synthesis and characterization of S-Ir-Gd:** The isostructural control heterobimetallic dyad **S-Ir-Gd** was synthesized and purified following the identical procedure described above for **S-Ir-Eu**, except that the mononuclear complex **S-Gd** was used instead of **S-Eu**. The final product was obtained as a yellow solid (C<sub>81</sub>H<sub>69</sub>F<sub>4</sub>GdIrN<sub>9</sub>O<sub>10</sub>, 53 mg, yield: 32%). HR-MS (positive mode,  $m/z$ ): Calcd. 1755.4047, found 1755.4025 for [(M+H)]<sup>+</sup>. Elemental Analysis: Calcd. C, 55.44; H, 4.02; N, 7.18, found C, 55.39; H, 3.98; N, 7.10.

[1] Z. Wang, L. Wang, S. Dong, C. Yang, J. Chen, W. Wang, G. Yang, Z. Han, "Rational Design of Rigid Chiral Ir(III)–Eu(III) Dyads: Intense Circularly Polarized Luminescence via Visible-Light Sensitization" *Inorg. Chem.* **2026**, *65*, 3209–3214.

[2] Z.-G. Niu, T. Zheng, Y.-H. Su, P.-J. Wang, X.-Y. Li, F. Cui, J. Liang, G.-N. Li, "Highly phosphorescent iridium( III ) complexes based on 2-(biphenyl-4-yl)benzo[d]oxazole derivatives: synthesis, structures, properties and DFT calculations" *New J. Chem.* **2015**, *39*, 6025–6033.

### Quantum Yield Determination

Luminescence quantum yields of **S-Ir-Eu** and **R-Ir-Eu** was determined in pure MeOH and DMSO with Ru(bpy)<sub>3</sub>Cl<sub>2</sub> (MeCN,  $\Phi=0.018$ ,  $\lambda=450$  nm, air-saturated) as a reference. The quantum yield was calculated using the following equation:

$$\Phi_S = \Phi_R \frac{F_S A_R n_S^2}{F_R A_S n_R^2}$$

Where  $\Phi_S$  and  $\Phi_R$  are the photoluminescence quantum yield of the sample and that of the reference.  $F_S$  and  $F_R$  are the corresponding integrated fluorescence intensity (areas) of sample and reference spectra, respectively.  $A_S$  and  $A_R$  are the absorbance of the sample and reference solution at the reference excitation wavelength.  $n_S$  and  $n_R$  are the solvent refractive indexes of the sample and reference. Absorbance of sample and reference at their respective excitation wavelength was controlled to be lower than 0.05.

### Cell lines and culture conditions

HeLa cells were cultured in DMEM medium supplemented with 10% FBS (fetal bovine serum) in an atmosphere of 5% CO<sub>2</sub> and 95% air at 37 °C. In each experiment, cells treated with vehicle control (1% DMSO) were kept as the reference group.

### Dark cytotoxicity assay

The *in vitro* dark cytotoxicity of **S-Ir-Eu** towards HeLa cell lines was determined by CCK-8 assay. Cells were seeded into a 96-well cell culture plate at  $1 \times 10^4$  per well, under 100% humidity, and were cultured at 37 °C with 5% CO<sub>2</sub> for 24 h. **S-Ir-Eu** in different concentrations (0.5, 1, 2, 5, 10, 30  $\mu$ M diluted in DMEM medium) were added into the wells. The cells were subsequently incubated for 24h at 37 °C under 5% CO<sub>2</sub>. After that, CCK-8 (10  $\mu$ L/well) was added to each well and the plate was incubated for an additional 4 h at 37 °C under 5% CO<sub>2</sub>. OD450 was monitored by an enzyme-linked immunosorbent assay reader (Thermo Scientific, Varioskan Flash).

### Photo-cytotoxicity test

HeLa cells were used to determine the photo-cytotoxicity of **S-Ir-Eu**. After 4 h incubation with **S-Ir-Eu** (0.5, 1, 2, 5, 10, 30  $\mu$ M diluted in DMEM medium), each well was washed three times with

the medium, and fresh medium was added to the wells. The cells were then exposed to a 450 nm laser irradiation for 300 s (diode laser,  $30 \text{ J}\cdot\text{cm}^{-2}$ ). After the irradiation, the cells were incubated for an additional 20 h at 37 °C under 5%  $\text{CO}_2$ . CCK-8 assay was conducted to measure the cell cytotoxicity.

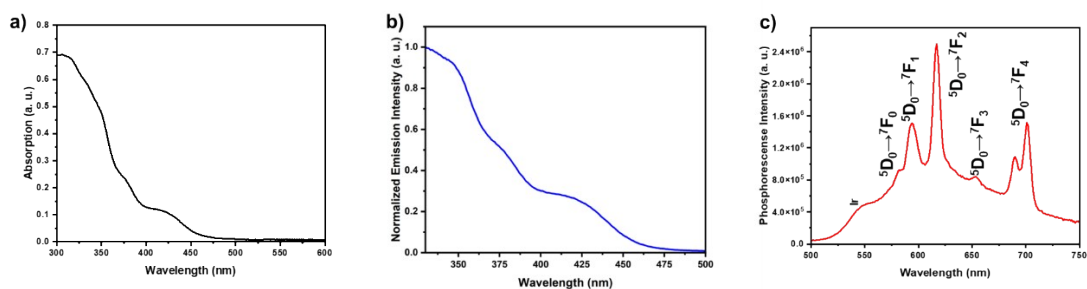


**Figure S1.** Absorption (a, 10  $\mu\text{M}$ ), excitation (b, 10  $\mu\text{M}$ ,  $\lambda_{\text{em}} = 616 \text{ nm}$ ) and emission spectra (c, 10  $\mu\text{M}$ ,  $\lambda_{\text{ex}} = 425 \text{ nm}$ ) of **R-Ir-Eu** in HEPES buffer containing 1 % DMSO, pH 7.4.

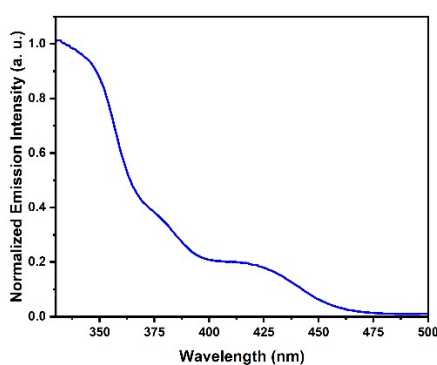


**Figure S2.** Excitation ( $\lambda_{\text{em}} = 616 \text{ nm}$ ) spectrum of **S-Ir-Eu** (10  $\mu\text{M}$ ) in HEPES buffer containing 1 % DMSO, pH 7.4.

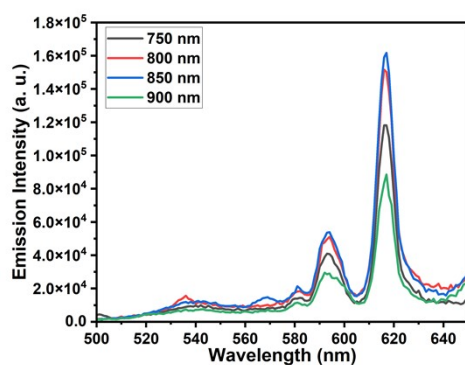


**Figure S3.** Emission spectrum of **S-Ir-Eu** (10  $\mu\text{M}$ ) in HEPES buffer containing 1 % DMSO, pH 7.4 under different two-photon excitation.

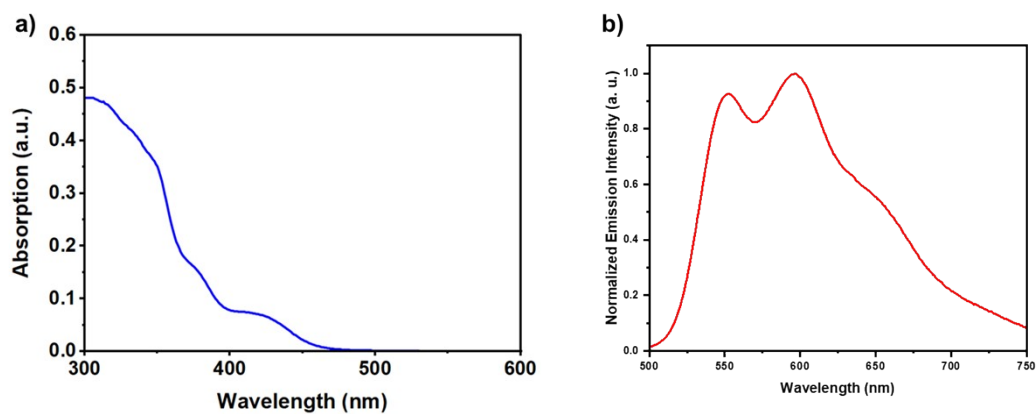


**Figure S4.** Absorption (a, 10  $\mu$ M) and emission spectra (c, 10  $\mu$ M,  $\lambda_{\text{ex}} = 425$  nm) of **S-Ir-Gd** in HEPES buffer containing 1 % DMSO, pH 7.4.

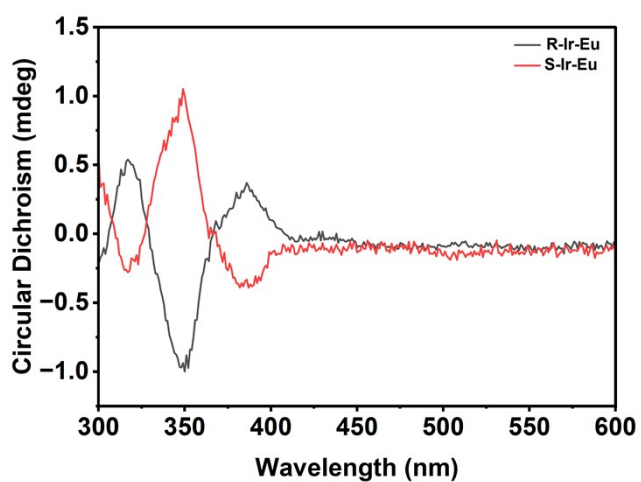


**Figure S5.** Circular dichroism (CD) spectra of **R-Ir-Eu** and **S-Ir-Eu** recorded in HEPES buffer containing 1% DMSO. Conditions: concentration = 10  $\mu$ M; temperature = 298 K.

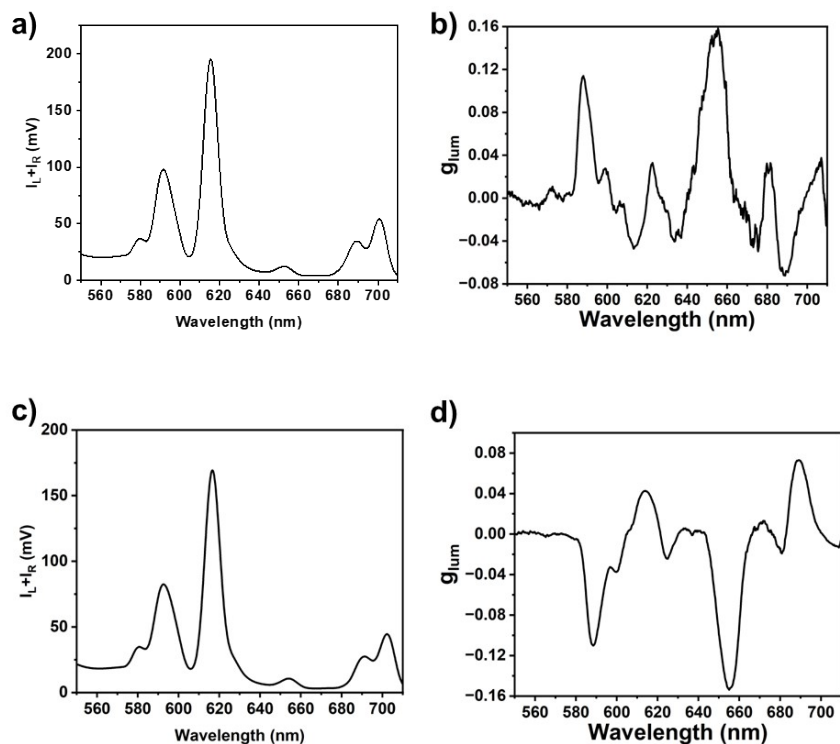


**Figure S6.** Total luminescence and  $g_{lum}$  spectra of **R-Ir-Eu** (a, b) and **S-Ir-Eu** (c, d) in MeOH under 425 nm excitation

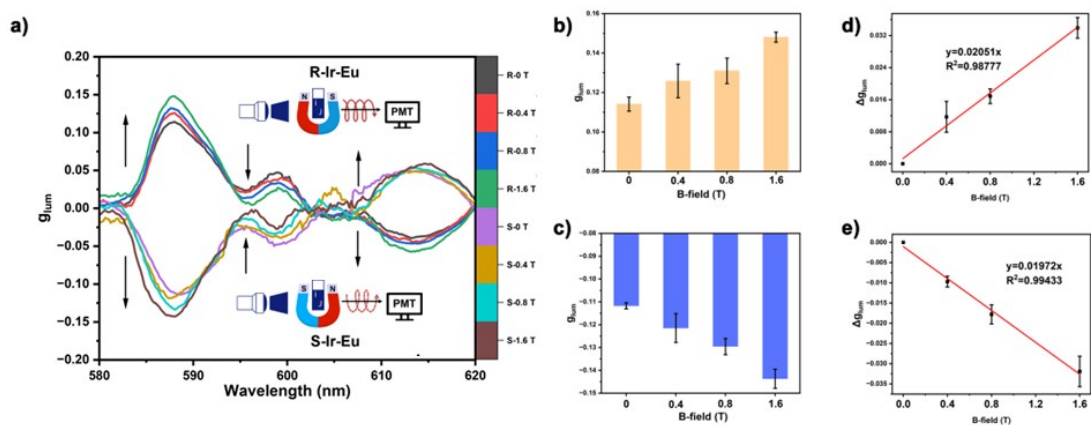


**Figure S7.** a) Magnetic field dependent  $g_{lum}$  spectra of **R-Ir-Eu** and **S-Ir-Eu** in HEPES buffer containing 1 % DMSO, pH 7.4, excited at 425 nm at room temperature, arrows indicate the trends of  $g_{lum}$  changes, inserted diagrams show the direction of applied magnetic field;  $g_{lum}$  and  $\Delta g_{lum}$  as a function of magnetic field strength at  $^5D_0 \rightarrow ^7F_1$  transition for **R-Ir-Eu** (b, d) and **S-Ir-Eu** (c, e).

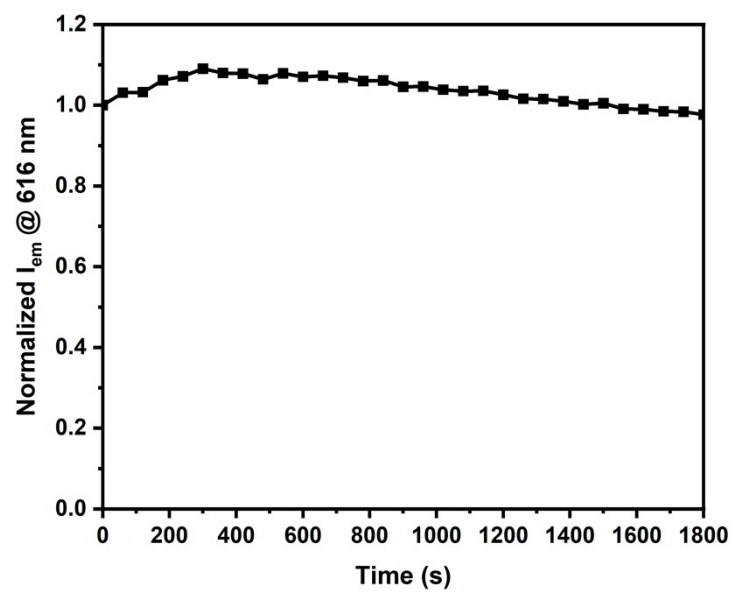


**Figure S8.** Photobleaching phosphorescence intensity of **S-Ir-Eu** (10  $\mu$ M) in HEPES buffer (pH 7.4, containing 1% DMSO, v/v) under continuous irradiation (425 nm).

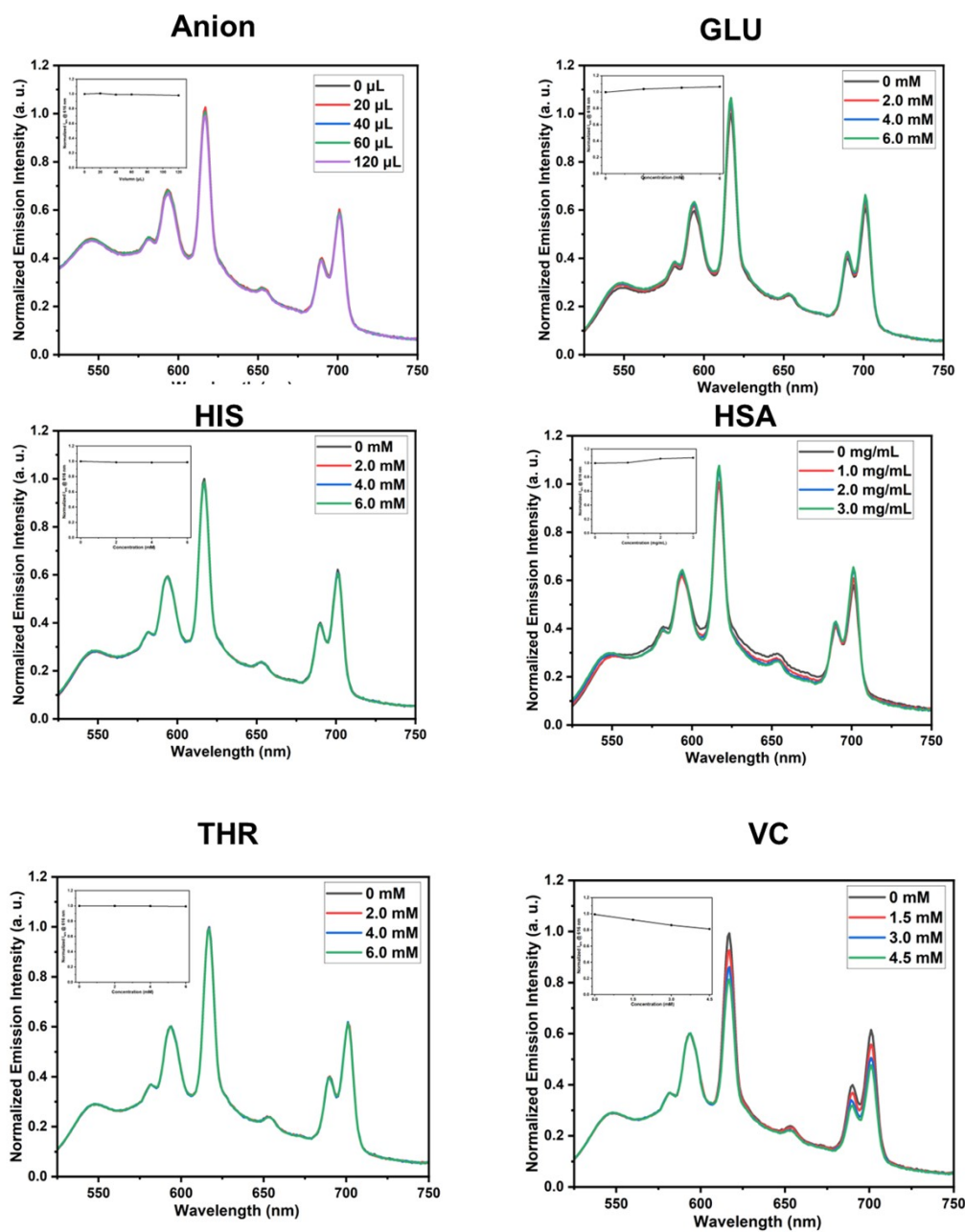


**Figure S9.** Emission spectra of S-Ir-Eu (10  $\mu$ M) in HEPES buffer containing 1 % DMSO, pH 7.4 under different physiological environments.

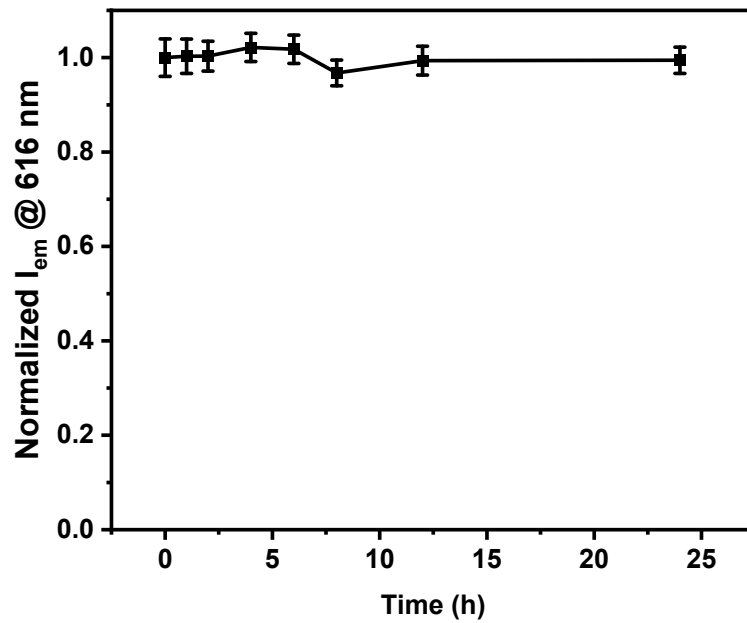


**Figure S10.** Serum-stability test of **S-Ir-Eu** (10  $\mu$ M) at 37  $^{\circ}$ C, showing the emission intensity @ 616 nm at different time points ( $\lambda_{\text{ex}}$ = 425 nm).

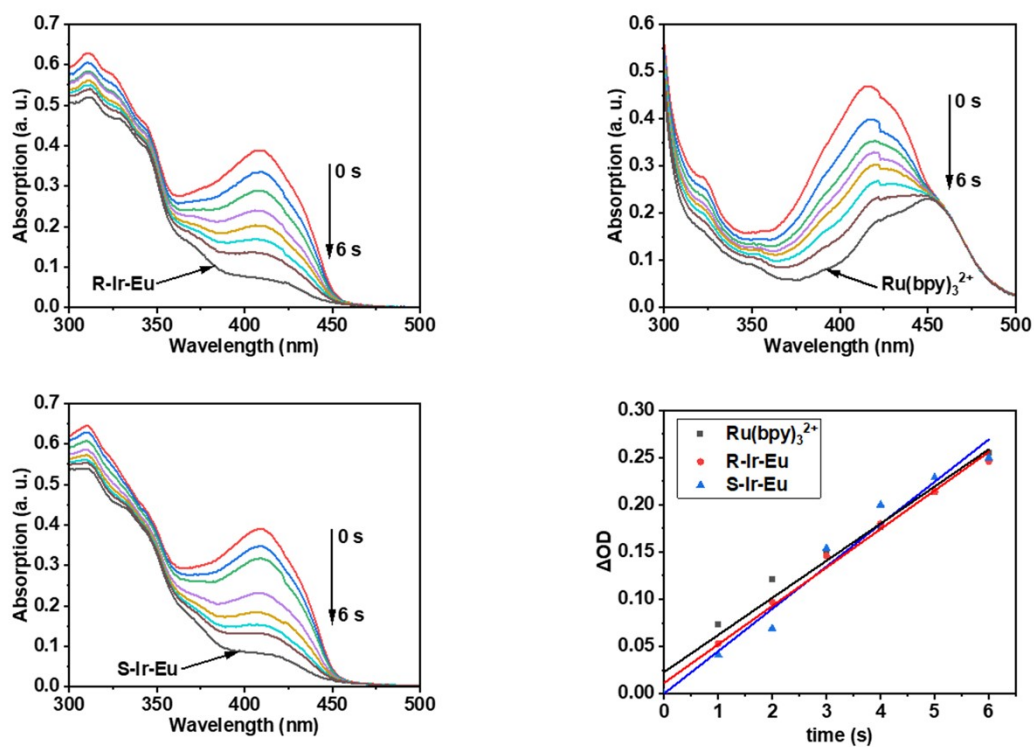


**Figure S11.** Changes in the absorption spectra of DPBF upon irradiation ( $\lambda = 450$  nm) with 1 s interval in the presence of **R-Ir-Eu** and **S-Ir-Eu**. The absorbance of complexes at the irradiation wavelength was adjusted to  $\sim 0.1$

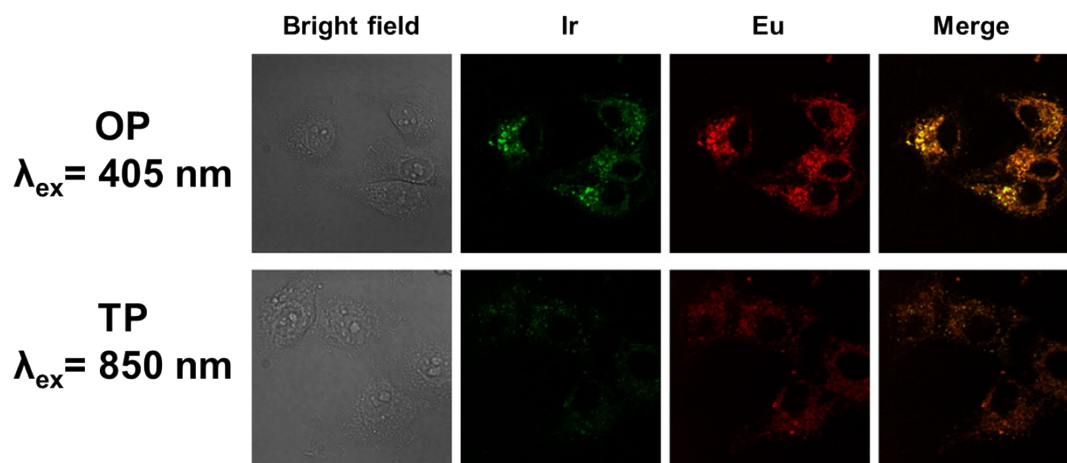


**Figure S12.** One and two photon confocal phosphorescence images of HeLa cells stained by **R-Ir-Eu** ( $20 \mu\text{M}$  in DMEM medium with 1% DMSO, 12 h). Scale bar:  $20 \mu\text{m}$ . Bandpaths: Ir (510-560 nm), Eu (580-620 nm).

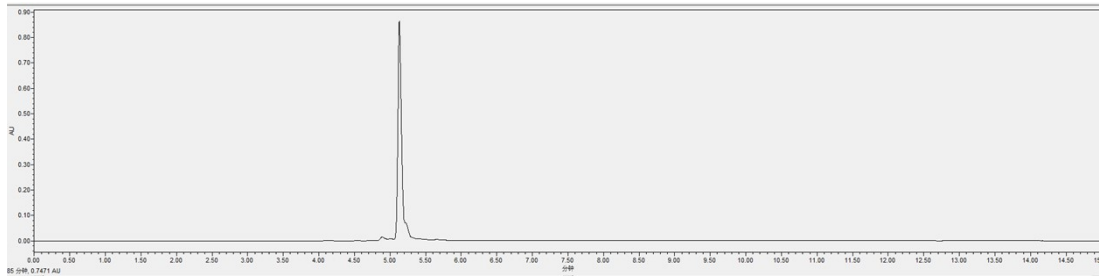
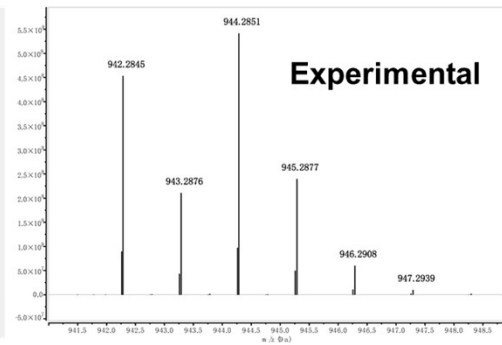
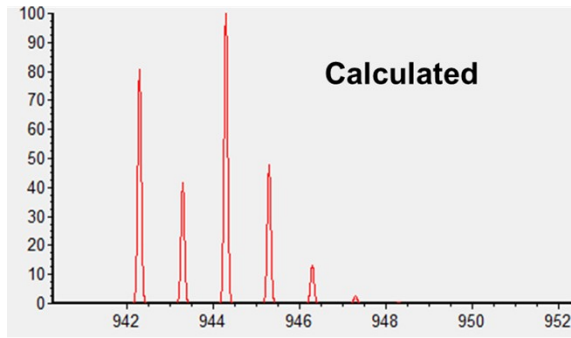
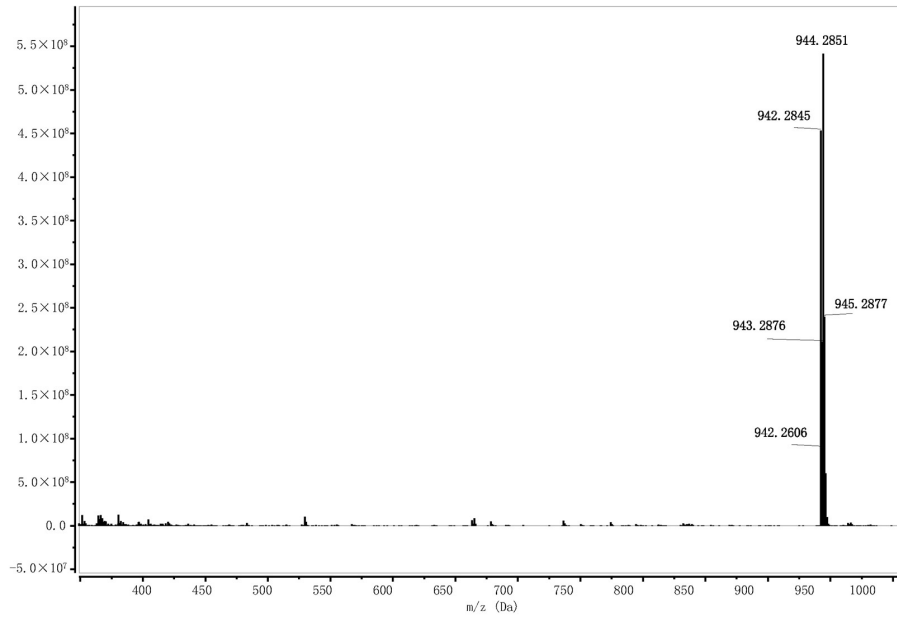


**Figure S13.** HR-MS and HPLC spectra of R-Eu

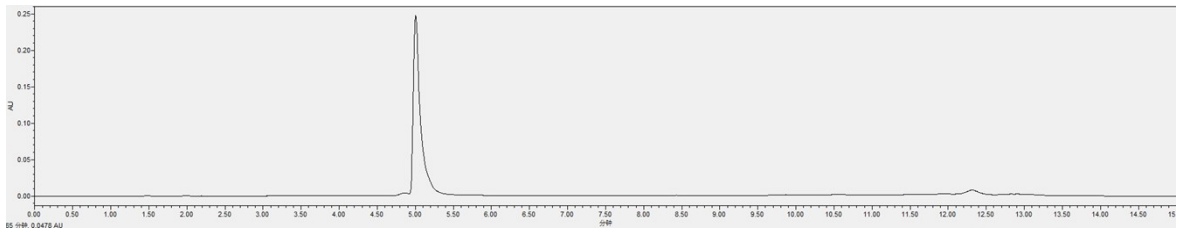
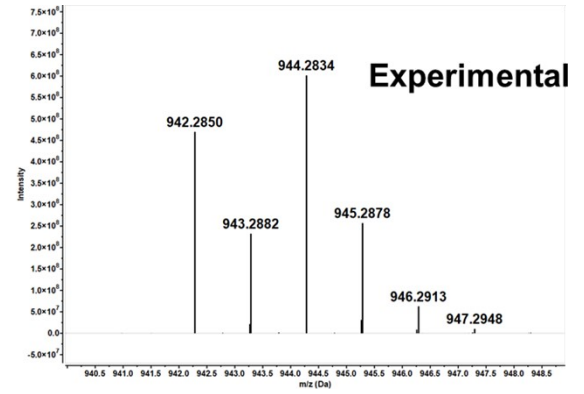
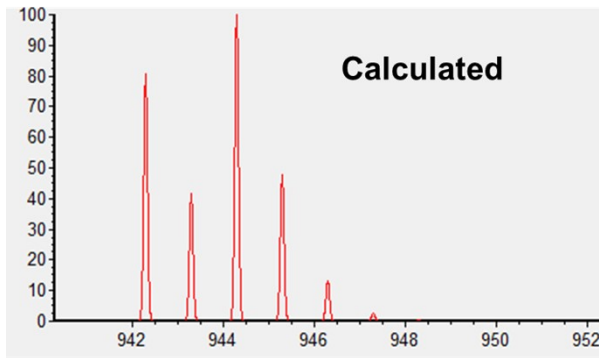
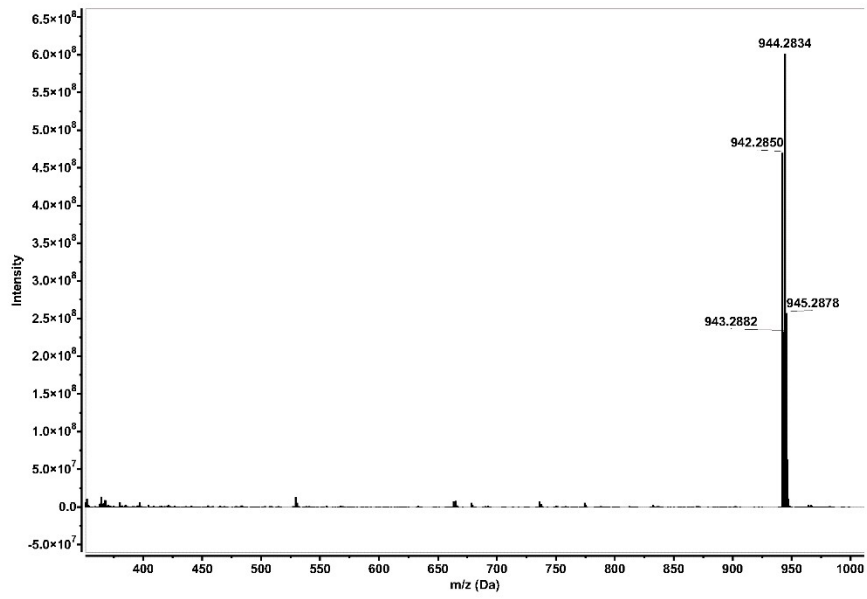


**Figure S14.** HR-MS and HPLC spectra of S-Eu

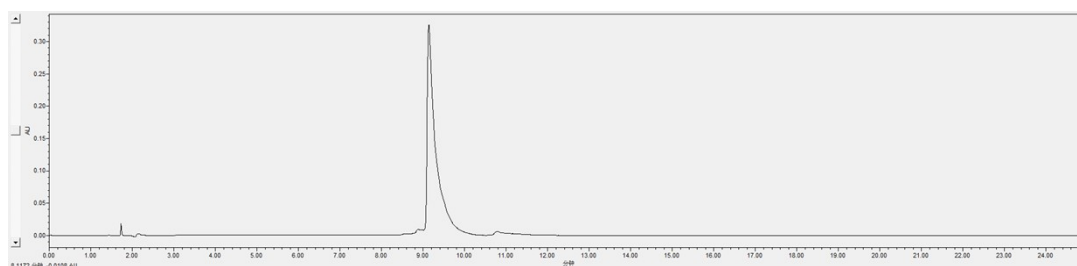
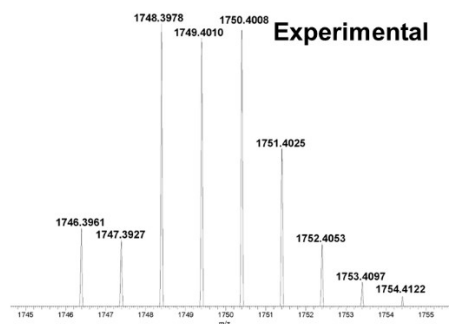
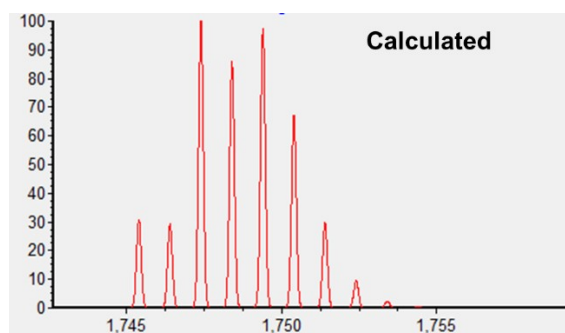
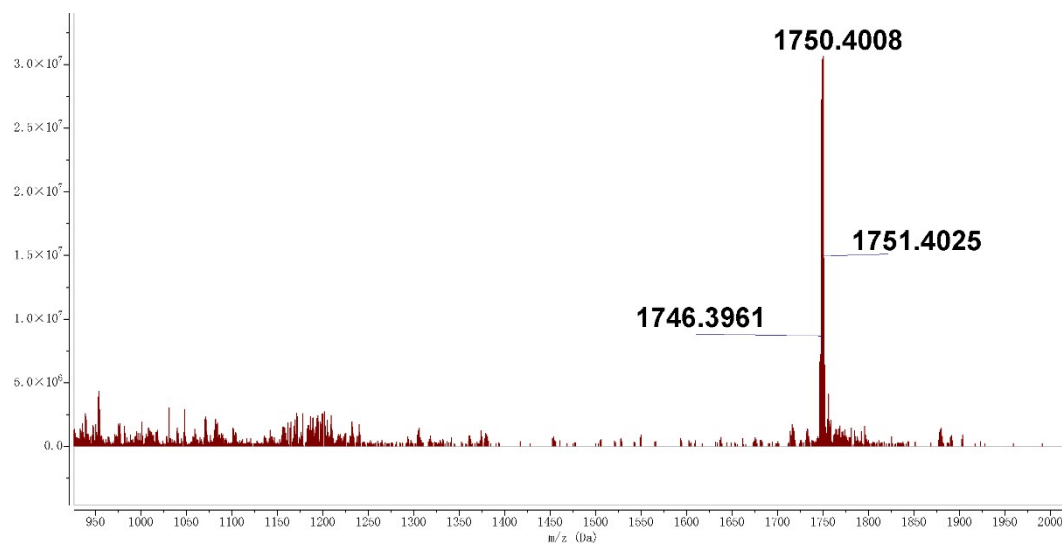


**Figure S15.** HR-MS and HPLC spectra of R-Ir-Eu

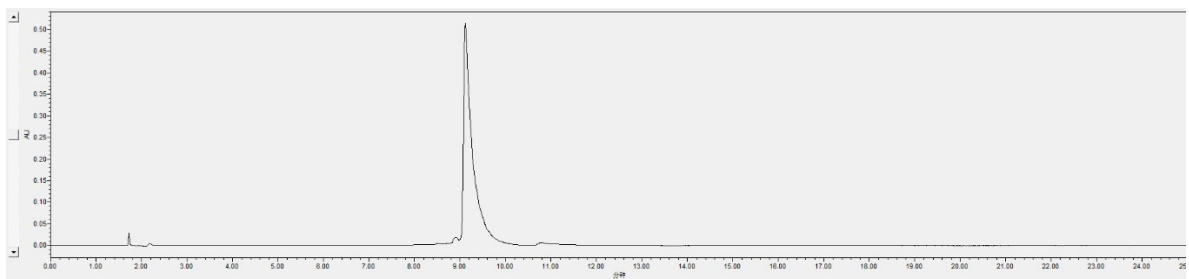
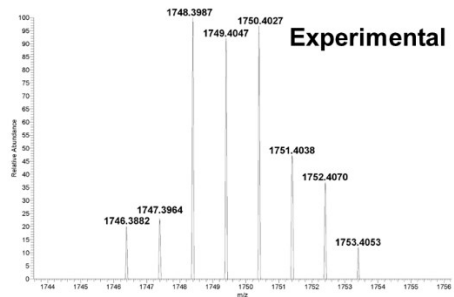
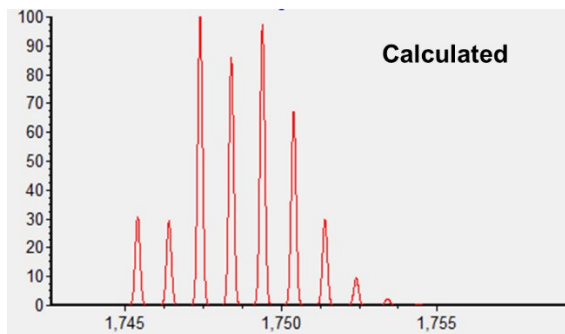
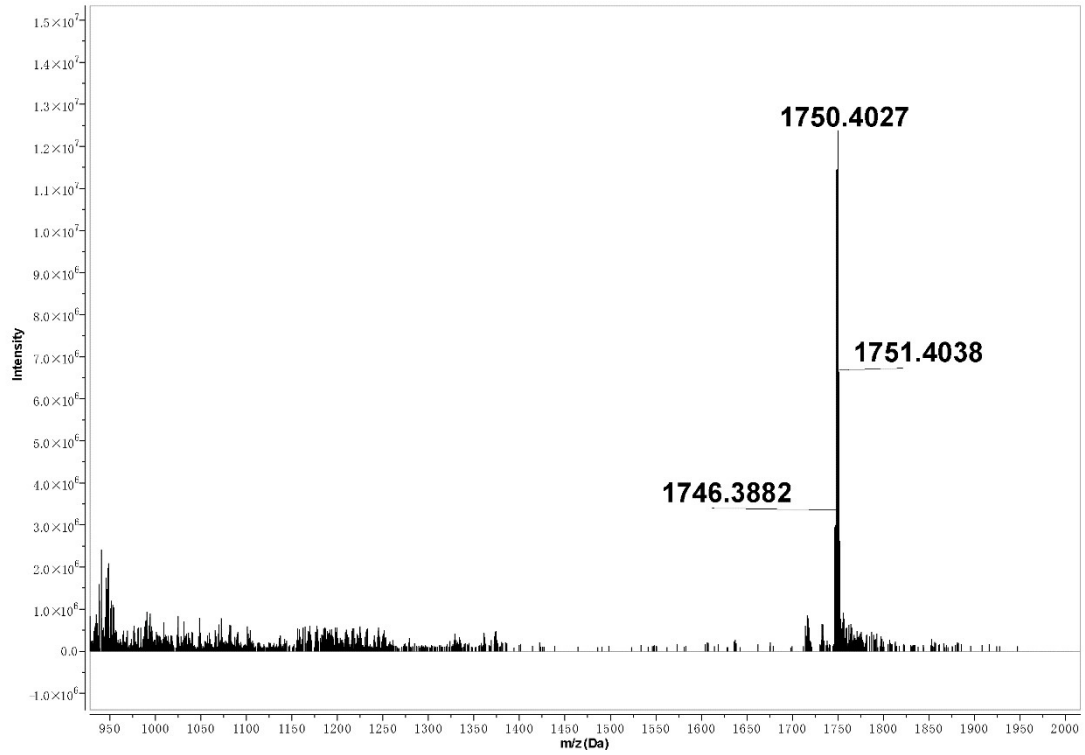
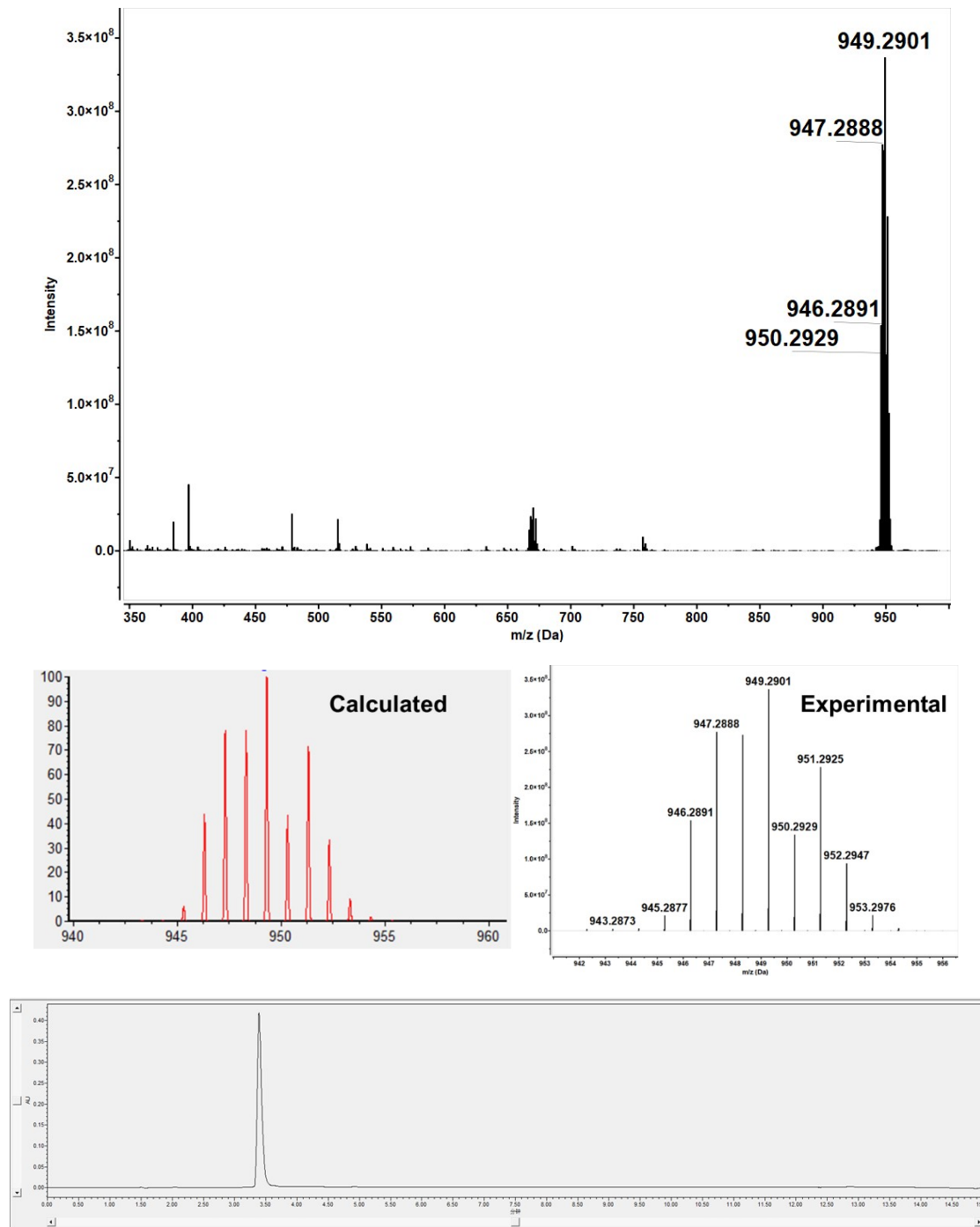


Figure S16. HR-MS and HPLC spectra of S-Ir-Eu



**Figure S17.** HR-MS and HPLC spectra of S-Gd

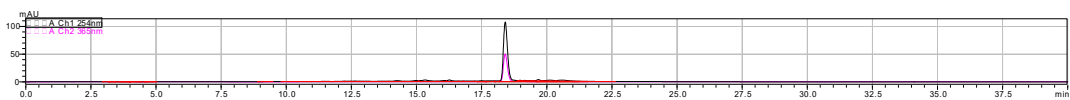
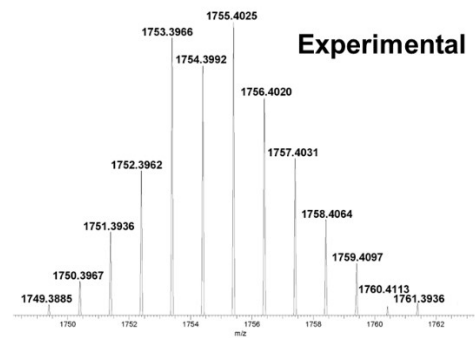
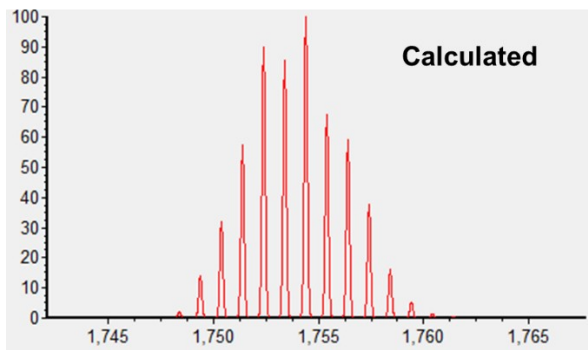
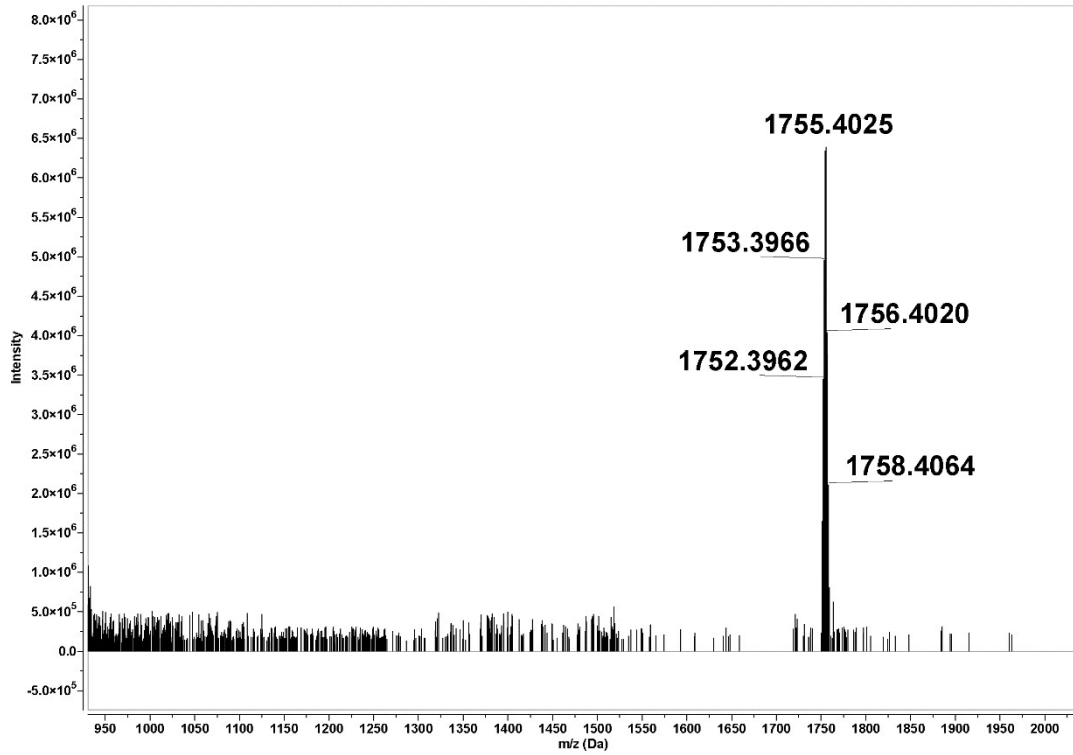


Figure S18. HR-MS and HPLC spectra of S-Ir-Gd

**Table S1. Photo-physical data of R-Ir-Eu and S-Ir-Eu**

|   | <b>R-Ir-Eu</b> | <b>S-Ir-Eu</b> |
|---|----------------|----------------|
| $\lambda_{\text{ex}}$ (nm) <sup>a</sup>       | 425            | 425            |
| R <sup>b</sup>                                | 1.56           | 1.56           |
| $\tau_{\text{MeOH}}$ ( $\mu\text{s}$ )        | 72.1           | 72.4           |
| $\tau_{\text{MeOD}}$ ( $\mu\text{s}$ )        | 74.3           | 74.5           |
| $\tau_{\text{DMSO}}$ ( $\mu\text{s}$ )        | 75.1           | 74.4           |
| $\tau_{\text{H}_2\text{O}}$ ( $\mu\text{s}$ ) | 69.2           | 70.1           |
| $\tau_{\text{D}_2\text{O}}$ ( $\mu\text{s}$ ) | 71.3           | 71.9           |
| $\Phi_{\text{MeOH}}$ (%) <sup>d</sup>         | 1.45           | 1.47           |
| $\Phi_{\text{DMSO}}$ (%) <sup>d</sup>         | 2.23           | 2.30           |
| q (Parker's, Horrocks') <sub>MeOH</sub>       | 0.19, 0.11     | 0.17, 0.09     |
| q (Parker's, Horrocks') <sub>H2O</sub>        | 0.21, 0.45     | 0.13, 0.37     |

<sup>a</sup> Absorption were recorded in HEPES (pH 7.4, containing 1% DMSO, v/v) at room temperature.

<sup>b</sup>  $I(^5\text{D}_0 \rightarrow ^7\text{F}_2)/I(^5\text{D}_0 \rightarrow ^7\text{F}_1)$

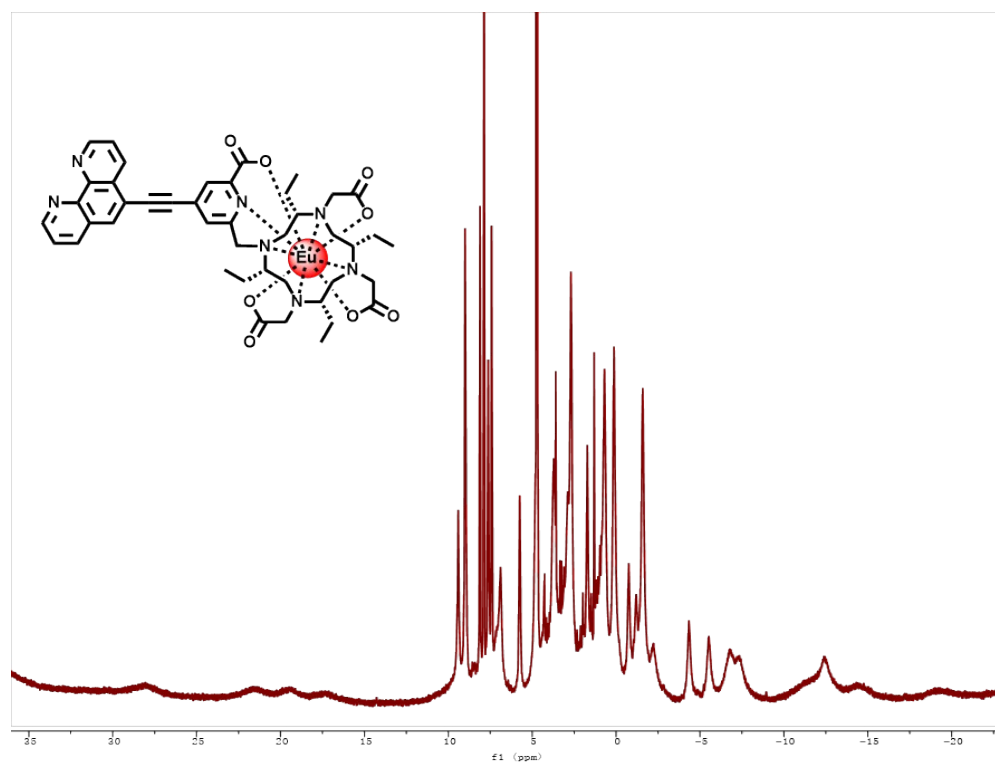
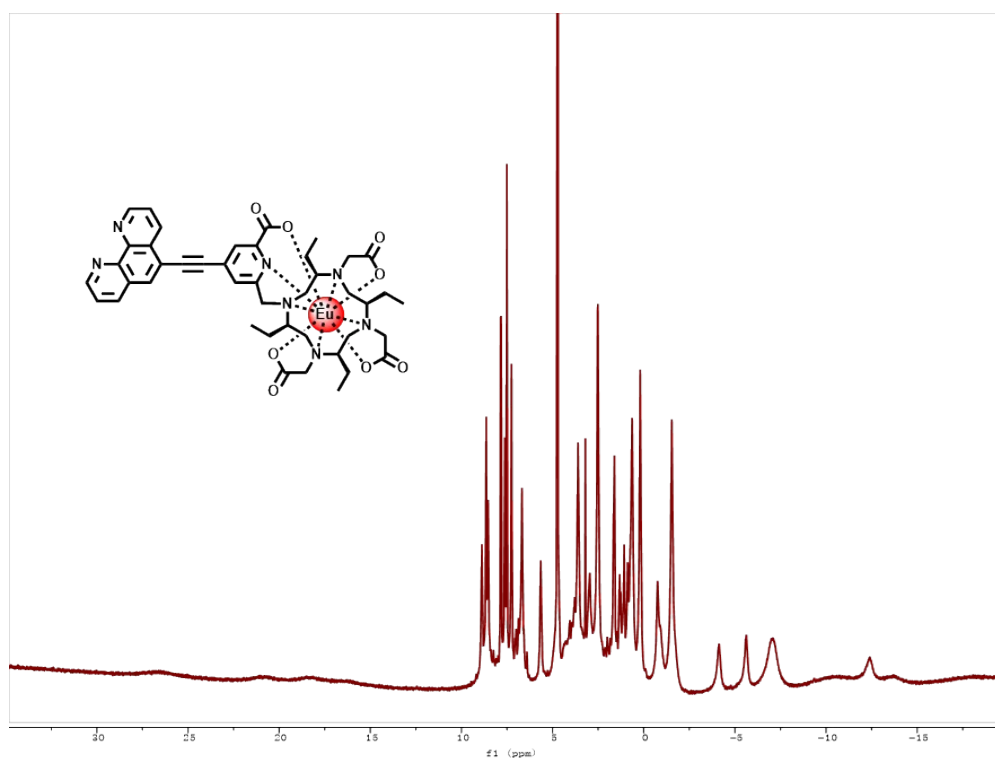
<sup>c</sup>  $\tau$  refers to the lifetime and was evaluated using TCSPC.

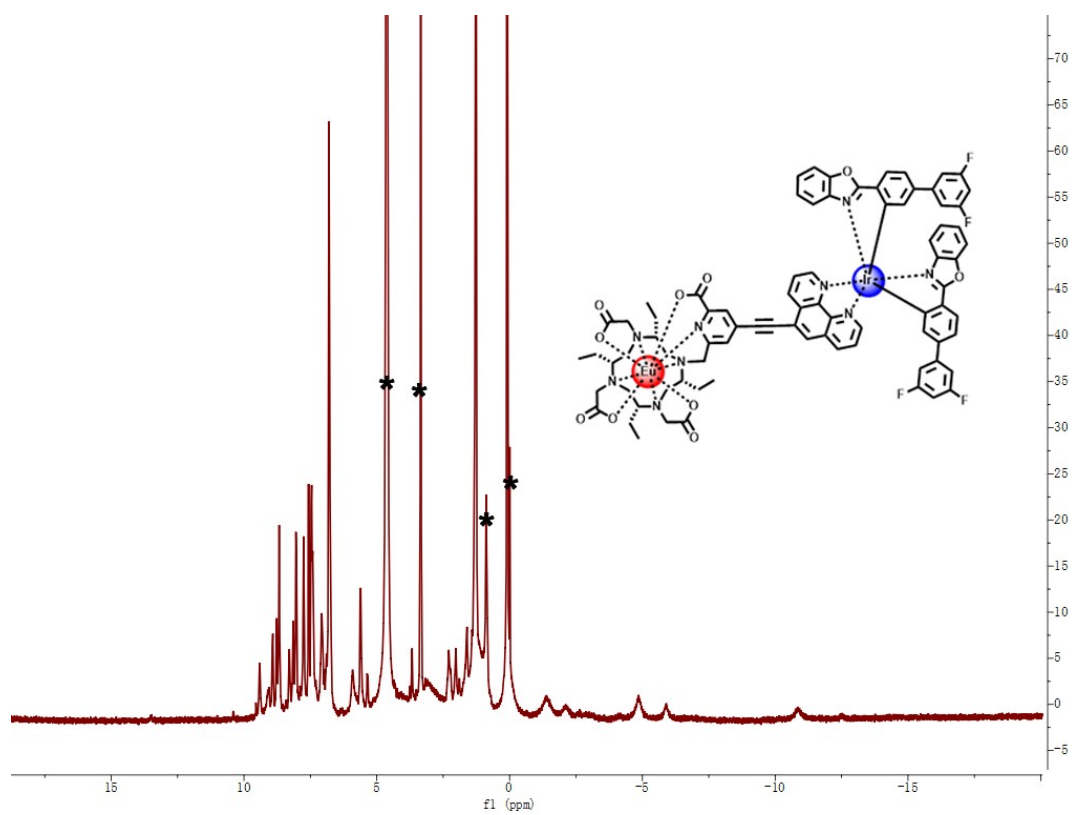
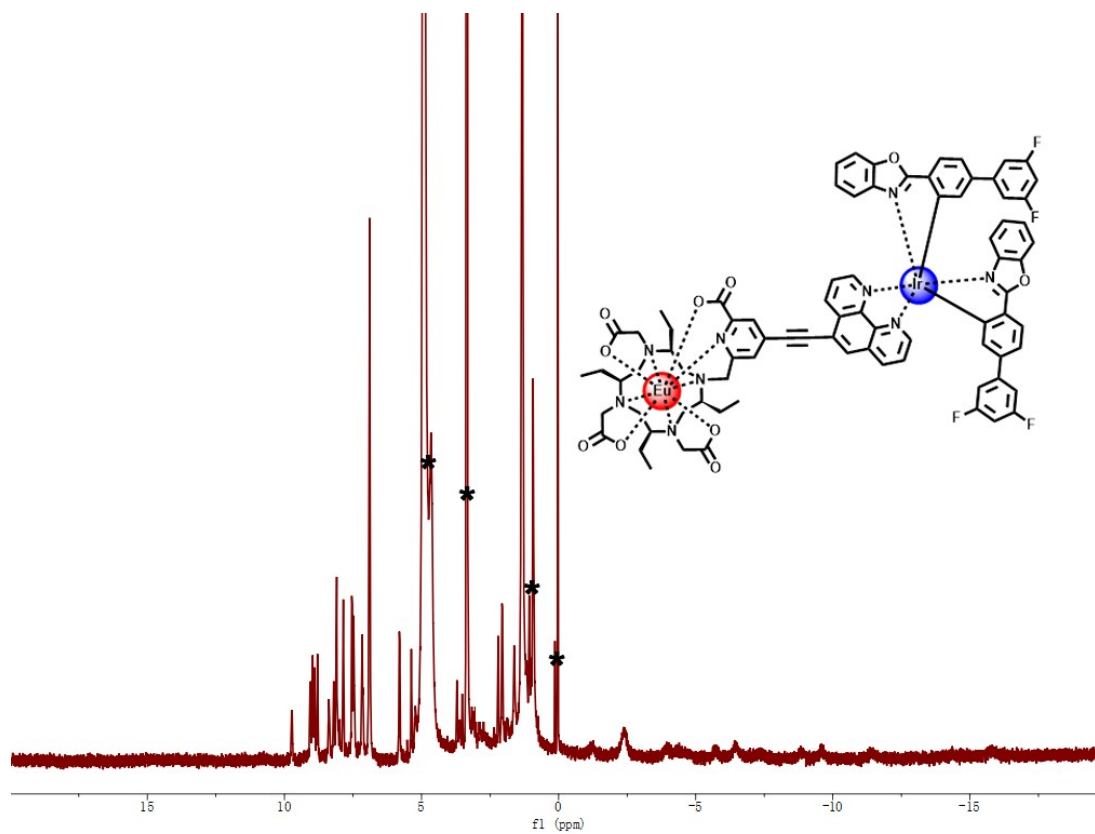
<sup>d</sup>  $\Phi$  refers to the luminescence quantum yield in air-saturated solvents, the standard used was Ru(bpy)<sub>3</sub>Cl<sub>2</sub> ( $\Phi=0.018$ ,  $\lambda=450$  nm, air-saturated acetonitrile).

**Table S2. Energy transfer kinetics of Ir-Gd-S and CPL complexes**

|                | $\tau$             | $\eta_{\text{EnT}}$ | $k_{\text{EnT}}$                  |
|----------------|--------------------|---------------------|-----------------------------------|
| <b>S-Ir-Gd</b> | 1.02 $\mu\text{s}$ | -                   | -                                 |
| <b>R-Ir-Eu</b> | 53 ns              | 94.8 %              | $1.79 \times 10^7 \text{ s}^{-1}$ |
| <b>S-Ir-Eu</b> | 50 ns              | 95.1 %              | $1.90 \times 10^7 \text{ s}^{-1}$ |

# NMR spectra





The asterisks (\*) stands for the residual, non-coordinating solvents (water, CD<sub>3</sub>OD, or laboratory grease).